

# A many-body GW+BSE investigation of electronic and optical properties of C<sub>2</sub>N

Jiuyu Sun,<sup>†</sup> Ruiqi Zhang,<sup>†</sup> Xingxing Li,<sup>†,‡</sup> and Jinlong Yang<sup>\*,†,‡</sup>

<sup>†</sup>*Hefei National Laboratory for Physical Sciences at the Microscale, University of Science  
and Technology of China, Hefei, Anhui 230026, China*

<sup>‡</sup>*International Center for Quantum Design of Functional Materials (ICQD), University of  
Science and Technology of China, Hefei, Anhui 230026, China*

E-mail: jlyang@ustc.edu.cn

Phone: +86-551-63606408. Fax: +86-551-63603748 (J. Y.)

ABSTRACT: A newly synthesized layered material  $C_2N$  was investigated based on many-body perturbation theory using  $GW$  plus Bethe-Salpeter equation approach. The electronic band gap was determined to be ranging from 3.75 to 1.89 eV from monolayer to bulk. Significant  $GW$  quasiparticle corrections, of more than 0.9 eV, to the Kohn-Sham band gaps from the local density approximation (LDA) calculations are found. Strong *excitonic effects* play a crucial role in optical properties. We found large binding energies of greater than 0.6 eV for bound excitons in few-layer  $C_2N$ , while it is only 0.04 eV in bulk  $C_2N$ . All the structures exhibit strong and broad optical absorption in the visible light region, which makes  $C_2N$  a promising candidate for solar energy conversion, such as photocatalytic water splitting.

**Keywords:** two-dimensional material,  $GW$ , Bethe-Salpeter equation, excitonic effect

## Introduction

Since the discovery of graphene,<sup>1</sup> two-dimensional (2D) and quasi-2D materials are of tremendous interest predominantly due to their extraordinary physical or chemical properties and great potential of application.<sup>2-5</sup> Graphitic  $C_3N_4$  (g- $C_3N_4$ ) has attracted much attention in recent years, for its high stability and moderate band gap, which can function as a metal-free polymeric photocatalyst for splitting water molecules with solar energy.<sup>6</sup> A new carbon nitride  $C_2N$  was also successfully synthesized most recently, which shows an optical gap of 1.96 eV and high on/off ratio of  $10^7$ .<sup>7</sup> The  $C_2N$  crystal is a layered structure with uniform holes and nitrogen atoms, as called ' $C_2N$ -h2D', which is composed of atomically thin  $C_2N$  monolayers [Fig. 1(a)] stacked by Van Der Waals interactions. Follow-up works suggest  $C_2N$  to be a promising metal-free photocatalyst for splitting water molecules with visible light by density functional theory (DFT) calculations<sup>8,9</sup> and a hydrogen evolution experiment.<sup>10</sup>

However, one cannot realistically envision  $C_2N$  devices until its fundamental excited-state properties, such as quasiparticle (QP) band and optical spectrum, are obtained. In

2D materials, Coulomb interactions between excited electrons and holes, i.e., *excitonic effects*, play a very important role in optical properties.<sup>11–17</sup> Quantum size confinement and less efficient electronic screening are two well-defined factors contributing to the excitonic effects.<sup>18</sup> Owing to its layered structure, C<sub>2</sub>N-*h*2D is expected to have strong excitonic effects too. Therefore, an appropriate description of the *e-e* correlation and *e-h* interaction is highly required to investigate the electronic and optical properties of C<sub>2</sub>N-*h*2D.

In the paper, we perform first-principles *GW* plus Bethe-Salpeter equation (BSE)<sup>19</sup> simulations to study the QP band structures and optical spectra of few-layer and bulk C<sub>2</sub>N-*h*2D. Firstly, the QP band gap of monolayer C<sub>2</sub>N enlarges from 1.7 eV (obtained by normal LDA calculations) to 3.75 eV, and due to strong excitonic effects, the lowest absorption peak is reduced to 2.75 eV compared to the electronic band gap. Secondly, the electronic band gaps, exciton binding energies, first bright excitonic energies (first optical absorption peaks) reduce with the increasing of the number of layers. Finally, strong optical absorptions in the visible light region were found for all structures from monolayer to bulk C<sub>2</sub>N-*h*2D. Our results suggest that few-layer C<sub>2</sub>N-*h*2D has better visible light absorption than graphitic C<sub>3</sub>N<sub>4</sub> (g-C<sub>3</sub>N<sub>4</sub>),<sup>20</sup> which makes C<sub>2</sub>N a promising candidate for metal free photocatalyst with enhanced solar energy conversion efficiency.

## Methods

In order to provide a good starting point for many-body calculations within the *GW* approximation, all the ground state of C<sub>2</sub>N structures were calculated using density functional theory (DFT) with local density approximation (LDA) functional as implemented in the QUANTUM ESPRESSO code.<sup>21</sup> The plane-wave cutoff was set as 50 RY with a norm-conserving pseudopotential. A  $10 \times 10 \times 1$  and  $8 \times 8 \times 6$  **k** grid was used for few-layered structures and bulk, respectively. The structures were fully relaxed until an energy convergence of  $10^{-9}$  RY and a force convergence on atoms of 0.01 eV/Å.

Starting from the wavefunction and energies of Kohn-Sham equations, the quasiparticle  $GW$  and BSE calculations were performed by using BerkeleyGW package.<sup>22</sup> A dynamical dielectric matrix within the random phase approximation (RPA) scheme and a generalized plasmon-pole model.<sup>23</sup> This gives rise to QP energy within a single-shot  $G_0W_0$  calculation. The involved unoccupied band number is up to more than 5 times of occupied band for every structure to achieve the converged dielectric function. The excitonic effects ( $e$ - $h$  interactions) are included by solving BSE with  $30 \times 30 \times 1$  and  $16 \times 16 \times 12$   $\mathbf{k}$  grids for few-layered structures and bulk, respectively.

## Results and discussion

### QP band structure

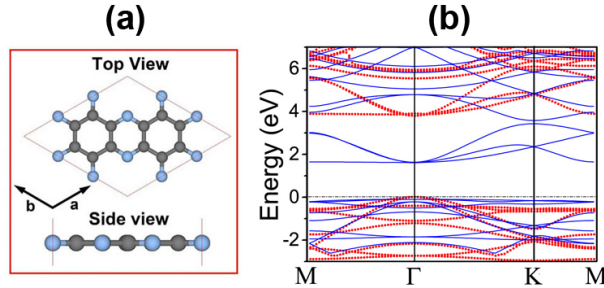


Figure 1: The (a) geometry structure and (b) band structure calculated by LDA (blue line) and  $GW$  (red dot) of monolayer  $C_2N$ - $h_2D$ . The grey and blue balls represent C atoms and N atoms, respectively.

The equivalent lattice parameter was optimized to 8.28 Å for monolayer  $C_2N$ - $h_2D$ , which is consistent to  $8.24 \pm 0.96$  Å by the experiment.<sup>7</sup> All of the band gap results calculated by DFT-LDA and  $GW$  method are shown in Table 1, as well as the results by HSE06.<sup>9</sup>

For monolayer  $C_2N$ - $h_2D$ , the direct band gap is located at  $\Gamma$  point. The band structures are shown in Figure 1(b). The energy gap calculated by  $GW$  is 3.75 eV, which is much greater than that by DFT-LDA (1.71 eV). Such large QP corrections to LDA eigenvalues are attributed to the enhance of  $e$ - $e$  interactions. This nonlocal behavior can not be correctly

**Table 1: The band gap energies  $E_g$  calculated by LDA, HSE06 and  $GW$  of monolayer, bilayer and bulk  $C_2N-h2D$ . For bulk, we listed  $E_g$  for both direct and indirect gaps.  $\Delta_1$  and  $\Delta_2$  were defined as:  $\Delta_1 = E_g^{HSE06} - E_g^{LDA}$  and  $\Delta_2 = E_g^{GW} - E_g^{LDA}$ , respectively. All values are in eV.**

	LDA	HSE06	$GW$	$\Delta_1$	$\Delta_2$
Monolayer	1.71	2.47	3.75	0.76	2.04
Bilayer	1.40	2.17	3.03	0.77	1.63
Trilayer	1.24	1.97	2.77	0.73	1.53
Bulk	1.11	1.81	2.07	0.70	0.96
	1.06 <sup>a</sup>	1.66 <sup>a</sup>	1.89 <sup>a</sup>	0.60	0.94

<sup>a</sup> Indirect band gap

described by LDA. However, HSE06 functional, having considered nonlocal exchange effects, results in a remarkably smaller gap than  $GW$  gap. Therefore the coulomb screening effect, which is only well described by self-energy operator in the  $GW$  scheme, plays a significant role in the electronic structure of monolayer  $C_2N-h2D$ . It is also noted that monolayer  $C_2N-h2D$  has comparable delocalized valence band maximum (VBM) and conduction band minimum (CBM) to g- $C_3N_4$ .<sup>20</sup> With a smaller direct gap,  $C_2N-h2D$  is suggested to have a better performance than g- $C_3N_4$  in light catalyst.

Regarding to bilayer, trilayer and bulk structures, we only considered the most stable stacking mode of AB-, ABC- and ABC-stacking,<sup>8</sup> respectively. All three band structures are performed in Figure 2. Direct band gaps at  $\Gamma$  point are found in bilayer and trilayer. Compared to monolayer, the QP band gaps decrease to 3.03 eV for bilayer and 2.77 eV for trilayer. This is because of the increasing coulomb screening effect, which is induced by quantum size confinement. However, it becomes an indirect gap for bulk (1.89 eV). The VBM occurs at  $\Gamma$  point. The CBM is located at A point (0.0 0.0 0.5) in Brillouin zone, which is 0.32 eV lower than CBM at  $\Gamma$ . The minimum direct band gap (2.21 eV) was located near (0 0 1/3) point.

For all the band structures of  $C_2N-h2D$ , there is no scissor operation for  $GW$  corrections in all the presented band structures. After considering nonlocal exchange interaction, several arched valence bands moves upward across the flat VBM in LDA, while the structures of

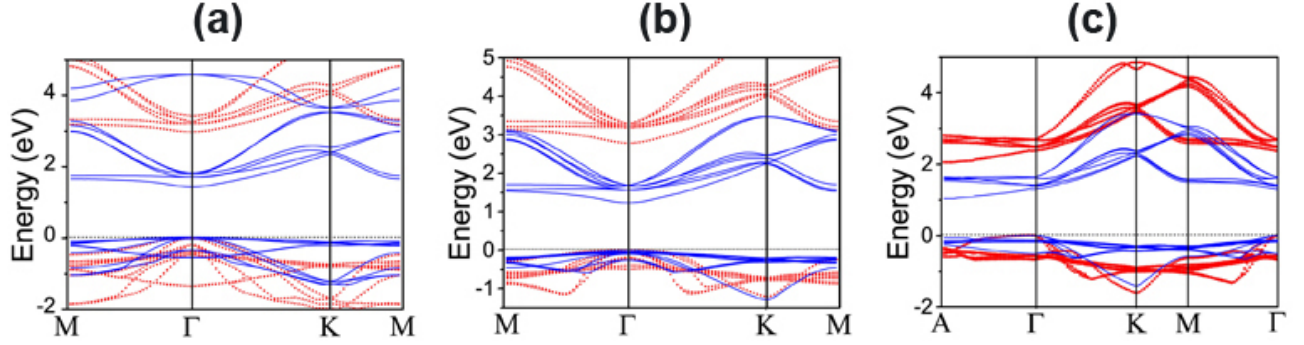


Figure 2: The band structures of (a) bilayer, (b) trilayer and (c) bulk  $C_2N-h2D$ . The band structures by LDA and  $GW$  are plotted by blue line and red dot, respectively.

conduction bands remain unchanged. The exchange correction induced change of VBM significantly enhances the carrier mobility for  $C_2N-h2D$ . Then we define the HSE06 and  $GW$  corrections to LDA band gap as  $\Delta_1$  and  $\Delta_2$ , respectively. As listed in Table 1,  $\Delta_1$  maintains about 0.7 eV for all the few-layered structures calculated. In contrast, as the number of layer increases,  $\Delta_2$  decreases rapidly from 2.04 eV (monolayer) to 1.53 eV (trilayer). This indicates that the correction of coulomb screening effects, unlike  $e-e$  exchange effects, depend deeply in the dimensional of the system. Thus,  $e-e$  interactions should be carefully treated when studying the electronic structure of few-layered  $C_2N-h2D$ . A power law fitting of the form  $(A/N^\alpha + B)$  is applied for  $GW$  calculated gaps, where  $N$  is the number of layers. It shows that the evolution of QP band gaps follows a  $1/N^{0.69}$  power law.

## Excitons and optical absorptions

In Figure 3(a) to (f), we performed optical absorption spectrum of few-layered  $C_2N-h2D$ . As shown in the figures, dramatic changes occur after  $e-h$  interactions are included ( $GW+BSE$ ). The optical absorptions are greatly modified and strongly bound exciton states well below the onset of single-particle transition continuum are indicated. There is an obvious cancellation effect between the band-gap opening due to the QP corrections and the redshift of optical absorption due to the strong excitonic effects.

In the case of monolayer, the first optically active (bright) exciton energies at 2.75 eV

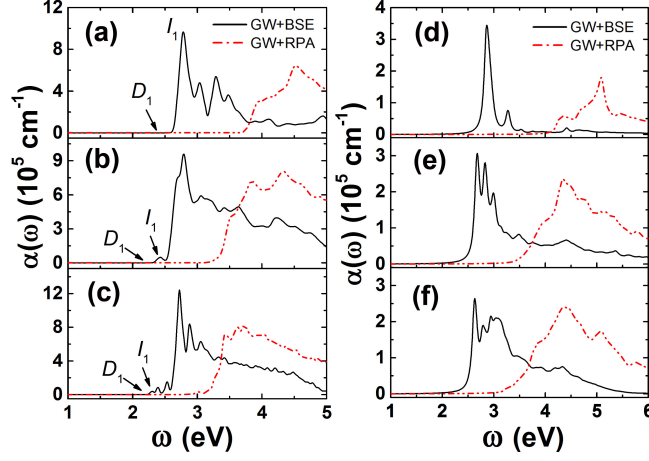


Figure 3: The absorption coefficient by  $GW+BSE$  (black line) and  $GW+RPA$  (red dash-dot) of (a, d) monolayer, (b, e) bilayer and (c, f) trilayer  $C_2N-h2D$  for light polarization parallel (left side) and perpendicular (right side) to the surface plane. A Gaussian broadening of 0.05 eV is adopted.

**Table 2:** First bright excitonic energies (optical gaps)  $E_{I1}$ , second excitonic energies  $E_{I2}$ , first dark excitonic energies  $E_D$  and binding energy of first bright excitons  $E_{I1}^b$  of monolayer, bilayer, trilayer and bulk  $C_2N-h2D$ . All values are in eV.

	$E_{I1}$	$E_{I2}$	$E_D$	$E_{I1}^b$
Monolayer	2.75	2.76	2.53	1.11
Bilayer	2.42	2.42	2.36	0.76
Trilayer	2.30	2.39	2.26	0.53
Bulk	2.02	2.17	-	0.04

( $I^1$ ) and the second one ( $I^2$ ) at 3.02 eV for light parallel to surface plane.  $I^1$  is in the nature of transitions from VBM to CBM at the  $\Gamma$  point. The binding energy  $E_b$  of the first exciton  $I^1$  is 1.11 eV. Such a large binding energy is due to the less efficient screening in monolayer structure. There are many optically inactive (dark) excitons. The first dark exciton was located at 2.53 eV ( $D^1$ ), dipole forbidden ( $10^{-6}$ ). These dark excitons may affect the luminescence yield in certain cases.

The optical absorption spectra of bilayer and trilayer of  $C_2N-h2D$  were performed in Figure 3(b) and (c), for light polarization parallel to the surface plane. Excitonic effects become weaker as the number of layers increasing. Comparing to monolayer, the red shifted of absorption of  $GW+BSE$  against  $GW+RPA$  is smaller than that in both cases of bilayer and trilayer  $C_2N-h2D$ . This indicates smaller binding energies of  $I^1$ . The absorption peaks of first light excitons of both structures are no longer as sharp as that in monolayer. With the increasing number of layers, intrinsic absorption begins to play a dominant role, instead of excitonic absorptions. For bilayer, the first two (doubly degenerated) optical bright exciton ( $I^1/I^2$ ) was located at 2.42 eV, with a binding energy of 0.76 eV. However, unlike monolayer and bilayer,  $I^1$  and  $I^2$  of trilayer are located at 2.30 eV and 2.39 eV, which exhibit two separate peaks in the spectra. As expected, the binding energy of  $I^1$  in trilayer reduced to 0.53 eV. Both  $I^1$  of bilayer and trilayer are excited from VBM to CBM near  $\Gamma$  point. In addition, the energies of two  $D^1$  are 2.36 eV and 2.26 eV eV for bilayer and trilayer, respectively. The dark excitons become stronger with dipoles in the magnitude of  $10^0$ , though there is no obvious corresponding peak in the absorption spectra.

It draws our highly attention that there are also strong excitonic effects in few-layered structures for light polarization perpendicular to the layer plane (see Fig. 3(d) to (e)). The first peak of monolayer was observed only a slight blue shift (0.1 eV) against the case for parallel polarized light. This is quite different to common 2D materials (see in supporting information), whose absorptions begin with the onset of single-particle transition (electronic band gap) for perpendicular polarized light. As shown in the figures, there are obvious red



shifts compared to absorptions without  $e$ - $h$  interactions for all the few-layered systems, indicating huge excitonic effects along the corresponding direction. Such a property makes few-layered  $C_2N$ - $h2D$  exhibits considerable absorptions of visible light along all the directions, which enhances the productivity of sunlight catalysis.

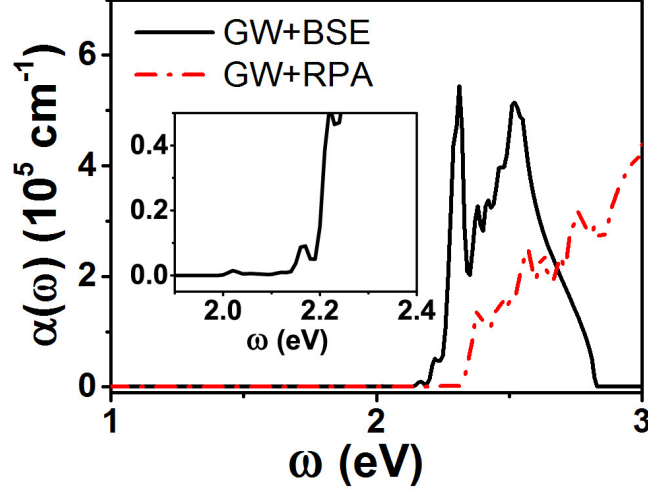


Figure 4: The absorption coefficient by  $GW+BSE$  (black line) and  $GW+RPA$  (red dash-dot) of bulk  $C_2N$ - $h2D$  for light polarization parallel to the surface plane. A Gaussian broadening of 0.01 eV is adopted.

In order to investigate how the excitonic effects are influenced by the quantum size confinement, we discuss the optical properties of bulk  $C_2N$ - $h2D$ , as the periodicity evolves from 2D to 3D. The optical absorption spectrum was presented in Figure 4 for light polarization parallel to the surface plane. There is no dark excitons in bulk  $C_2N$ . The energy of first bright exciton is 2.02 eV, with a binding energy of 0.04 eV. This value is in agreement with the experimentally optical gap (1.96 eV) for layered crystal containing more than 10 layers. It should be pointed out that the indirect interband transitions of electrons were not concerned in the present study, which may slightly red shift the absorption peak. The  $I^1$  transition from VBM to CBM takes place near the  $\mathbf{k}$  point  $(0\ 0\ 1/3)$  along  $\Gamma$  to A, which is consistent with the minimum QP band direct gap point just discussed above. The second excitonic peak is located at 2.14 eV with a binding energy of 0.02 eV. Such small binding energies indicate that excitons in bulk  $C_2N$  are typical Mott-Wannier excitons.

A power law fitting of the same form is applied for excitonic energies of  $I^1$  (optical gap). The evolution of optical gaps follows a  $1/N^{0.90}$  power law, which means a faster reduction than QP band gap. An empirical formula

$$E_b = 0.21 * E_{gap} + 0.4 \quad (1)$$

was proposed by Ref.,<sup>24</sup> which shows a linear law between  $E_b$  and QP band gap  $E_{gap}$  for 2D materials. For monolayer our calculated  $E_b$  is in good agreement with Equation 1, while  $E_b$  of bilayer and trilayer are at least 0.3 eV smaller than those predicted according to the empirical formula. The failure of Eq. 1 is mainly attributed to their assumption that macroscopic dielectric constant  $\epsilon$  of layered structures equals to 1. However, owing to the enhanced screening effects in multi-layered structures,  $\epsilon$  varies significantly with the increasing thickness from quasi-2D to 3D.<sup>25</sup> Thus the relationship between  $E_{gap}$  and  $E_b$  for multilayer systems is no longer simple linear law.

## Conclusion

In summary, we investigated electronic and optical properties of monolayer, bilayer and bulk  $C_2N$ - $h2D$  by using  $GW+BSE$  methods. Large quasiparticle band gap corrections to LDA were found in all the calculated structures. By comparing to the results of HSE06 functional, it shows a deeply dependence of coulomb correlation interactions on the number of layers, while exchange interactions are almost unchanged. In layered structures, strong excitonic effects play a crucial role in optical properties, with a significant large binding energy assigned to bound excitons. As the structure evolves from monolayer to bulk, the leading role of excitonic optical absorptions becomes weaker. Different to common 2D materials,  $C_2N$ - $h2D$  exhibits comparable excitonic effects in both directions for light polarization parallel and perpendicular to the layer plane. Excitons in bulk turn to Mott-Wannier excitons with small binding energies. The optical gap of bulk  $C_2N$  is in agreement with the result by the

experiment. As a result of quantum size confinement, quasiparticle band gaps and optical gaps reduce with the increase of layer number ( $N$ ), following  $1/N^{0.69}$  and  $1/N^{0.90}$  power law respectively. Absorptions in region of visible light are found for all the layered and bulk  $C_2N$ . We suggest layered  $C_2N$ - $h$ 2D may have extraordinary electronic and optical properties, especially for visible light catalysis.

## Acknowledgement

This work is partially supported by the National Key Basic Research Program (2011CB921404), the NSFC (21421063, 91021004, 21233007), by CAS (XDB01020300), and by USTCSCC, SCCAS, Tianjin, and Shanghai Supercomputer Centers.

## References

- (1) Novoselov, K. S.; Geim, A. K.; Morozov, S. V.; Jiang, D.; Zhang, Y.; Dubonos, S. V.; Grigorieva, I. V.; Firsov, A. A. Electric field effect in atomically thin carbon films. *Science* **2004**, *306*, 666–669.
- (2) Trevisanutto, P. E.; Giorgetti, C.; Reining, L.; Ladisa, M.; Olevano, V. Ab Initio GW Many-Body Effects in Graphene. *Physical Review Letters* **2008**, *101*, 226405–226408.
- (3) Malko, D.; Neiss, C.; Viñes, F.; Görling, A. Competition for Graphene: Graphynes with Direction-Dependent Dirac Cones. *Physical Review Letters* **2012**, *108*, 086804–086808.
- (4) Splendiani, A.; Sun, L.; Zhang, Y.; Li, T.; Kim, J.; Chim, C. Y.; Galli, G.; Wang, F. Emerging photoluminescence in monolayer MoS<sub>2</sub>. *Nano Lett* **2010**, *10*, 1271–1275.
- (5) Steinkasserer, L. E.; Gaston, N.; Paulus, B. Weak interactions in Graphane/BN systems under static electric fields-A periodic ab-initio study. *J Chem Phys* **2015**, *142*, 154701.
- (6) Wang, X.; Maeda, K.; Thomas, A.; Takanabe, K.; Xin, G.; Carlsson, J. M.; Domen, K.; Antonietti, M. A metal-free polymeric photocatalyst for hydrogen production from water under visible light. *Nat Mater* **2009**, *8*, 76–80.

- (7) Mahmood, J.; Lee, E. K.; Jung, M.; Shin, D.; Jeon, I.-Y.; Jung, S.-M.; Choi, H.-J.; Seo, J.-M.; Bae, S.-Y.; Sohn, S.-D. et al. Nitrogenated holey two-dimensional structures. *Nature Communications* **2015**, *6*, 6486–6492.
- (8) Zhang, R.; Li, B.; Yang, J. Effects of stacking order, layer number and external electric field on electronic structures of few-layer C<sub>2</sub>N. *Nanoscale* **2015**, *7*, 14062–14070.
- (9) Zhang, R.; Li, B.; Yang, J. Bilayer C<sub>2</sub>N Nanosheet: A Promising Metal-free Photocatalyst for Water Splitting. *arXiv: 1505.02584* **2015**,
- (10) Mahmood, J.; Jung, S.-M.; Kim, S.-J.; Park, J.; Yoo, J.-W.; Baek, J.-B. Cobalt Oxide Encapsulated in C<sub>2</sub>N-2D Network Polymer as a Catalyst for Hydrogen Evolution. *Chemistry of Materials* **2015**, *27*, 4860–4864.
- (11) Yang, L. Excitonic effects on optical absorption spectra of doped graphene. *Nano Lett* **2011**, *11*, 3844–3847.
- (12) Yang, L.; Deslippe, J.; Park, C.-H.; Cohen, M. L.; Louie, S. G. Excitonic Effects on the Optical Response of Graphene and Bilayer Graphene. *Physical Review Letters* **2009**, *103*, 186802–186805.
- (13) Cudazzo, P.; Attaccalite, C.; Tokatly, I. V.; Rubio, A. Strong Charge-Transfer Excitonic Effects and the Bose-Einstein Exciton Condensate in Graphane. *Phys. Rev. Lett.* **2010**, *104*, 226804–226807.
- (14) Arnaud, B.; Lebègue, S.; Rabiller, P.; Alouani, M. Huge Excitonic Effects in Layered Hexagonal Boron Nitride. *Physical Review Letters* **2006**, *96*, 026402–026405.
- (15) Qiu, D. Y.; da Jornada, F. H.; Louie, S. G. Optical Spectrum of MoS<sub>2</sub>: Many-Body Effects and Diversity of Exciton States. *Physical Review Letters* **2013**, *111*, 216805–216809.
- (16) Tran, V.; Soklaski, R.; Liang, Y.; Yang, L. Layer-controlled band gap and anisotropic excitons in few-layer black phosphorus. *Physical Review B* **2014**, *89*, 1–6.
- (17) Shu, H.; Li, Y.; Wang, S.; Wang, J. Thickness-Dependent Electronic and Optical Properties of Bernal-Stacked Few-Layer Germanane. *The Journal of Physical Chemistry C* **2015**, 15526–15531.
- (18) Yang, L.; Cohen, M. L.; Louie, S. G. Excitonic Effects in the Optical Spectra of Graphene Nanoribbons. *Nano Letters* **2007**, *7*, 3112–3115.

- (19) Rohlfing, M.; Louie, S. G. Electron-hole excitations and optical spectra from first principles. *Physical Review B* **2000**, *62*, 4927–4944.
- (20) Wei, W.; Jacob, T. Strong excitonic effects in the optical properties of graphitic carbon nitride g-C<sub>3</sub>N<sub>4</sub> from first principles. *Physical Review B* **2013**, *87*, 085202–085208.
- (21) Giannozzi, P.; Baroni, S.; Bonini, N.; Calandra, M.; Car, R.; Cavazzoni, C.; Ceresoli, D.; Chiarotti, G. L.; Cococcioni, M.; Dabo, I. et al. QUANTUM ESPRESSO: a modular and open-source software project for quantum simulations of materials. *J Phys Condens Matter* **2009**, *21*, 395502–395520.
- (22) Deslippe, J.; Samsonidze, G.; Strubbe, D. A.; Jain, M.; Cohen, M. L.; Louie, S. G. BerkeleyGW: A massively parallel computer package for the calculation of the quasiparticle and optical properties of materials and nanostructures. *Computer Physics Communications* **2012**, *183*, 1269–1289.
- (23) Hybertsen, M.; Louie, S. Electron correlation in semiconductors and insulators: Band gaps and quasiparticle energies. *Physical Review B* **1986**, *34*, 5390–5413.
- (24) Choi, J.-H.; Cui, P.; Lan, H.; Zhang, Z. Linear Scaling of the Exciton Binding Energy versus the Band Gap of Two-Dimensional Materials. *Physical Review Letters* **2015**, *115*, 066403–066407.
- (25) Latini, S.; Olsen, T.; Thygesen, K. S. Excitons in van der Waals heterostructures: The important role of dielectric screening. *Physical Review B* **2015**, *92*, 245123–245135.